Biochimica et Biophysica Acta 860 (1986) 215–228
Elsevier

BBA 73225

Fluorescence studies of the incorporation of *N*-(7-nitrobenz-2-oxa-1,3-diazol-4-yl)-labeled phosphatidylethanolamines into liposomes

Tudor Arvinte [a], Amelia Cudd [b] and Knut Hildenbrand [a,*]

[a] *Max-Planck-Institut für Strahlenchemie, Stiftstrasse 34, D-4330 Mülheim-Ruhr (F.R.G.) and* [b] *Centre de Biophysique Moléculaire du C.N.R.S., F-45071 Orleans Cedex 2 (France)*

(Received February 28th, 1986)

Key words: Lipid-membrane interaction; Fluorescent label incorporation; Unilamellar vesicle; Kinetics; Membrane reorganization; ^{31}P-NMR; Electron microscopy

The kinetics of interaction of aqueous suspensions of phosphatidylethanolamine derivatives with single bilayer egg yolk phosphatidylcholine (egg PC) vesicles has been studied. For this purpose 7-nitrobenz-2-oxa-1,3-diazol-4-yl (NBD) was reacted with the free amino group of L-α-phosphatidylethanolamine, -dilauroyl and -dimyristoyl to give *N*-NBD-DLPE (Ia) and *N*-NBD-DMPE (Ib). Electron microscopy and ^{31}P-NMR experiments performed with (Ia) indicated that the labeled lipids in aqueous buffer are present in the form of nonbilayer aggregates of 100–200 Å diameter with a highly disordered headgroup arrangement. The time-evolution of the NBD emission intensity in the incubation mixtures of (I) with small and large unilamellar vesicles (SUV and LUV) could be fitted with a double exponential function. The fluorescence decay parameters of the NBD group changed during the reaction time of (I) with SUV but did not change when aggregates of (I) were mixed with LUV. A kinetic model was evaluated which assumes the adsorption of aggregates of (I) to the surface of the liposomes in a primary step. The relaxation characteristics of this heterogeneous lipid distribution towards a more homogeneous membrane structure can be explained by the presence of two non-fluorescent pools of (I) and a fluorescent one in the egg PC matrix. The rate constants for transfer of (I) between those kinetic pools as well as equilibrium emission intensities were found to decrease with increasing length of the fatty acid chains of (I). This behaviour was explained by differences in the properties of the clusters of (I) in the egg PC membranes.

Introduction

In order to apply fluorescence techniques to membrane research (see Ref. 1), suitable organic molecules have to be either dissolved in the bilayers or covalently attached to polar or apolar regions of phospholipids. While artificial membranes can be readily labeled by cosonication of the fluorescent compounds with the matrix lipids, the incorporation of the fluorescent probes into biological membranes is more complicated. Normally, the membranes are incubated with an aqueous solution or suspension of the label molecules and loosely bound probe molecules are removed by washing. For example, this method has been used for the incorporation of diphenylhexatriene

* To whom correspondence should be addressed.

Abbreviations: ANS, 1-anilino-8-naphthalenesulfonate; DLPE, dilauroyl-L-α-phosphatidylethanolamine; DMPE, dimyristoyl-L-α-phosphatidylethanolamine; egg PC, egg yolk phosphatidylcholine; NBD, 7-nitrobenz-2-oxa-1,3-diazol-4-yl; NMR, nuclear magnetic resonance; PE, phosphatidylethanolamine from egg yolk; SUV, small unilamellar egg PC vesicles; LUV, large unilamellar egg PC vesicles; EM, electron microscopy; TLC, thin-layer chromatography.

into cell membranes [2], for the incorporation of intramolecular excimer probes such as dipyrenylpropane into erythrocyte ghost membranes [3] and into sarcoplasmic reticulum [4], and for the incorporation of *N*-NBD-PE into erythrocyte ghost membranes [5]. Whereas the spectroscopic properties of the label molecule in membrane regions have been extensively studied, information concerning the mechanisms of incorporation of these molecules into lipid bilayers is limited to a few cases. It was shown, e.g., that the incorporation of small molecules like 1-anilino-8-naphthalenesulfonate (ANS) [6–9] as well as that of a pyrene-labeled phospholipid [10] into lipid membranes follow biphasic kinetics. Rapid initial adsorption of the amphiphatic molecules to the membrane surface followed by a slow penetration into the membrane interior were assumed to be the reason for the complex kinetics. In the present paper the mechanism of interaction of aqueous suspensions of two *N*-NBD-labeled lipids (Scheme I) with egg PC single bilayer membranes was studied, for the following reasons mainly: (i) the

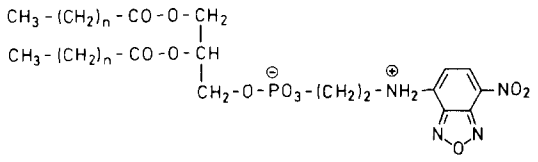

(Ia) n = 10 ; N-NBD-DLPE
(Ib) n = 12 ; N-NBD-DMPE

Scheme I. Structural formulae of *N*-NBD-DLPE and *N*-NBD-DMPE.

compounds (I) show fluorescence properties which make them especially suited for kinetic experiments using emission techniques. They are practically non-fluorescent in aqueous suspension, they emit with high quantum yield when dissolved in membranes in concentrations of less than 0.5 mol% and they show strong self-quenching when incorporated in higher concentrations or when aggregated in lipid domains [11]. (ii) NBD-labeled lipids are widely used to study spontaneous transfer of lipids [12–14] and fusion of membranes [15–18] by resonance energy transfer methods as well as lateral lipid diffusion by fluorescence recovery after photobleaching (FRAP) [5]. Therefore, thorough knowledge of their incorporation into lipid membranes is of importance for practical purposes. (iii) Besides the importance for technical applications these results can be seen from a more general point of view. A kinetic model has been evaluated which involves the formation of membrane structures showing lipid distributions far from equilibrium. The fluorescence measurements presented here give information on the kinetics of membrane reorganization which is not accessible by conventional fluorescence labeling experiments.

In this connection it was the influence of the hydrophobic part of compounds (I) which attracted our attention. It is well-known that the structure of the hydrophobic lipid part is dominating not only structural and dynamic properties of membranes but also the rates of exit and entry of lipids from and into bilayers. While the short chain lipid (Ia) is readily transferred between SUV with a half-time of 37 min [12] we detected no transfer of the homologous compound (Ib) for incubation times as long as 12 h. Therefore, it seemed pertinent to ask whether similar differences could be obtained for the incorporation of the compounds (I) into lipid membranes.

Materials and Methods

Chemicals

NBD chloride was purchased from Fluka. *N*-NBD-ethanolamine was from Molecular Probes and *n*-octyl glucoside from Sigma.

Lipids

Egg PC, grade 1, and PE from egg yolk, grade 1, were purchased from Lipid Products, DLPE was from Fluka and DMPE from Sigma. NBD-labeled lipids were prepared and purified as described in Ref. 12. The compounds were characterized by ^{1}H-NMR spectroscopy at 90 or 400 MHz ($T = 23°C$, solvent: dimethylsulfoxide-d_6). The covalently attached NBD group gave rise to the following parameters: δ 8.60 (d, 1 H, $J = 9.0$ Hz), δ 6.51 (d, 1 H, $J = 9.0$ Hz); (the corresponding data for NBD chloride under the same conditions are: δ 8.78 (d, 1 H, $J = 7.6$ Hz), δ 8.11 (d, 1 H, $J = 7.6$ Hz). The signals of the fatty acid chains were observed at δ 1.30 (s, 40 H for (Ia), 44 H (Ib) (methylene)) and δ 0.94 (m, 6 H, methyl).

The labeled lipids were kept as a stock solution in $CHCl_3$/MeOH under Ar. Concentrations of the labeled phospholipids ($CHCl_3$/MeOH) were determined from the absorbance using a value of $\varepsilon = 6.4 \cdot 10^4\ M^{-1} \cdot cm^{-1}$ for the molar absorption coefficients of NBD at 460 nm [19]. The lipids showed single spots on TLC in the solvent mixture $CHCl_3$/MeOH/H_2O (65 : 24 : 4, v/v).

Preparation of vesicles

Small unilamellar vesicles (SUV) were prepared by sonicating 30 mg of egg PC or 30 mg of mixtures of (I) and egg PC (molar ratio of 0.5 : 100) in 3 ml of 10 mM potassium phosphate buffer containing 80 mM NaCl (pH 7.8). Sonication was performed with a Branson Sonifier B15 for 20 min under Ar at 4°C. The SUV were separated from aggregates and multilamellar liposomes by passage through a Sepharose 4B column [20].

Large unilamellar vesicles (LUV) were obtained by detergent removal using a 1 ml Lipoprep dialysis cell [21]. The starting mixtures contained 10 mg egg PC and 20 mg *n*-octyl glucoside in 1 ml buffer (10 mM potassium phosphate/80 mM NaCl (pH 7.8)). The pore-size of the dialysis membranes provided a molecular mass cut-off at 10 kDa. According to Refs. 20 and 21 the diameters of the SUV and LUV are 250 Å and 1800 Å, respectively. From the dimension of the vesicles and a surface area of approx. 70 $Å^2$ of egg PC [22] the total number of lipid molecules in SUV and LUV were estimated to be 6000 and 240000, respectively.

Preparation of N-NBD-lipid aggregates

For fluorescence measurements, an aliquot of the stock solution of (I) was evaporated to dryness under Ar and exposed to high vacuum for 2 h. Buffer (10 mM phosphate/80 mM NaCl (pH 7.8)) was added to the resulting film. The suspension was sonicated for 5 min with a Branson Sonifier B15 at maximum power until the lipid film was removed from the glass wall. For fluorescence measurements, the concentration of the labeled lipids was $5 \cdot 10^{-7}$ M.

Characterization of aggregates of N-NBD-labeled phosphatidylethanolamines

Electron microscopy of N-NBD-DLPE aggregates. For negative staining, aliquots from suspensions of NDB-lipid aggregates in 10 mM Tris-HCl buffer (pH 7.4, $5.2 \cdot 10^{-5}$ M lipid concentration), prepared by sonication as described, were placed on collodion-covered grids, negatively stained with ammonium molybdate (pH 7.4) and examined using a Siemens Elmiskop 102 electron microscope. The diameters of individual aggregates were calculated from photographs printed at 4-times negative enlargements, multiplying the measured aggregate diameter by 0.707, in the assumption that the measured surfaces represent disc surfaces resulting from collapsed spherical aggregates.

To prepare inclusions of NBD-lipid aggregates, more concentrated suspensions in 10 mM Tris-HCl buffer at pH 7.4 ($2.4 \cdot 10^{-3}$ M lipid concentration) were mixed with warm agar (Difco, 2% in 10 mM Tris-HCl, pH 7.4). 1 mm^3 pieces of the hardened mixture were incubated at 0–4°C in a solution of 3% glutaraldehyde (Polysciences Inc.) in 0.1 M sodium cacodylate buffer (pH 7.4) containing 0.03% $CaCl_2$. After washing at 0–4°C in a solution of 0.3 M saccharose in 0.1 M sodium cacodylate buffer (pH 7.4), containing 0.03% $CaCl_2$, the agar cubes were incubated at 0–4°C with a solution of 2% OsO_4 (Polysciences Inc.) in 0.1 M sodium cacodylate buffer, 0.15 M saccharose, 0.03% $CaCl_2$ and then dehydrated using an ethanol gradient. The dehydrated agar cubes were included in Epon (Polysciences Inc.). Thin sections on copper grids were stained with uranyl acetate and examined.

^{31}P-NMR spectroscopy. Proton-noise decoupled ^{31}P-NMR spectra of egg PC, DLPE and (Ia) were obtained at 36.42 MHz with a Bruker WH 90 NMR spectrometer. The temperature was kept at 32°C. Normally, 100000 free induction decays were accumulated employing a 60° pulse, a 12000 Hz sweep width and a delay time of 0.4 s. The samples were prepared in the following way: 10 mg of lipid in $CHCl_3$ solution was added to a flask. The solvent was evaporated under Ar followed by exposure to high vacuum for 2 h. The lipid film was hydrated in 0.3 ml of buffer (10 mM Tris-HCl, 80 mM NaCl and 10% ^2H_2O at pH 7.0) and transferred to a 5 mm NMR tube under Ar.

Fluorescence measurements. Sample preparation. In a typical experiment, aggregates of (I)

($5 \cdot 10^{-7}$ M) were prepared as described above and mixed in the fluorescence cell at zero time with unlabeled vesicles (10^{-4} M lipid concentration) under Ar. The cell was sealed afterwards with a Teflon stopcock to minimize exposure to oxygen during the measurements.

Steady-state fluorescence measurements were performed on a Perkin-Elmer LS 5 spectrofluorometer in a thermostated sample holder. NBD was excited at 475 nm. For kinetic measurements the emission intensity was monitored at the emission maximum of NBD ($\lambda_{em} = 530$ nm). In order to compensate for instrumental fluctuations during the measurements, emission intensities were calibrated with respect to a standard sample (10^{-6} M *N*-NBD-ethanolamine in ethanol). The fluorescence intensities were insensitive to gentle manual shaking of the sample. Thus it may be assumed that artifacts due to membrane aggregation and settling of fluorescent materials were insignificant.

Normalization of emission intensities. Steady-state emission intensities (F) of the incubation mixtures of (I) with SUV and LUV, of cosonicated systems and of pelleted samples were normalized to the emission intensities of the samples after treatment with Triton X-100 (1% v/v final concentration). Control experiments had shown that the mean lifetimes and the steady-state emission intensities of the Triton treated samples were independent of the hydrophobic part of (I) and of the vesicle size.

Fluorescence lifetimes were determined by the time-correlated single-photon counting method. The nanosecond fluorescence spectrometer was equipped with a PRA nanosecond flash lamp (C25) filled with N_2 at approx. 350 torr. Excitation and emission wavelengths of 354 nm and 535 nm, respectively, were selected by interference filters of 20 nm bandwidth. A quartz wedge scrambler plate in the excitation path and a film polarizer set at 35.3° relative to the vertical direction in the emission beam provided magic angle geometry. The data were collected in an Ortec 6220 multichannel analyzer and transferred to a VAX 11/780 computer. Deconvolution and data fitting according to

$$F(t) = \sum_{i=1}^{j} \alpha_i \, e^{-t/\tau_i} \quad (j = 1 \text{ and } 2) \qquad (1)$$

was accomplished by an iterative deconvolution method. The quality of the fit was judged by both a reduced χ^2 criterion and a plot of weighted residuals [23]. Mean lifetimes $\langle \tau \rangle$ (for $j = 2$) were calculated from the decay times τ_i and preexponentials α_i using Eqn. 2 [24]

$$\langle \tau \rangle = (\alpha_1 \tau_1^2 + \alpha_2 \tau_2^2)/(\alpha_1 \tau_1 + \alpha_2 \tau_2) \qquad (2)$$

Lifetime measurements at various reaction times in the incubation mixtures of (I) with LUV and SUV were collected during time intervals of 5–10 min. Despite the poor signal-to-noise ratio obtained under these conditions it was possible to perform satisfactory fits of the data and to resolve two decay components.

Ultracentrifugation. Characterization of the size-distribution of aggregates of (I) and information on the extent of association of *N*-NBD-labeled lipids with LUV was obtained by centrifugation with a Beckman L5-65 ultracentrifuge for 1 h at $100\,000 \times g$ (SW 60 Ti rotor, $T = 20$°C). The pellets were washed with buffer and centrifuged a second time. Control experiments showed that less than 15% of the aggregates of (I) and approx. 50% of the LUV were pelletable under those conditions.

Results

The goal of the present study was to obtain information on the mechanisms of the incorporation of *N*-NBD-labeled phosphatidylethanolamines into membrane bilayers. In a typical experiment an aqueous suspension of the labeled PE was mixed with a suspension of egg PC vesicles at zero time. Changes in emission intensities and fluorescence lifetimes of the NBD-moiety were used to study the mechanism of the interaction of the two components of the mixture. It is obvious that for an interpretation of these experiments the NBD aggregates must be characterized properly. For this purpose several procedures were used:

(a) Electron microscopy

As indicated in Materials and Methods two different EM techniques were applied:

(1) EM micrographs of inclusions of the lipid aggregates in Epon are shown in Fig. 1. The heavy

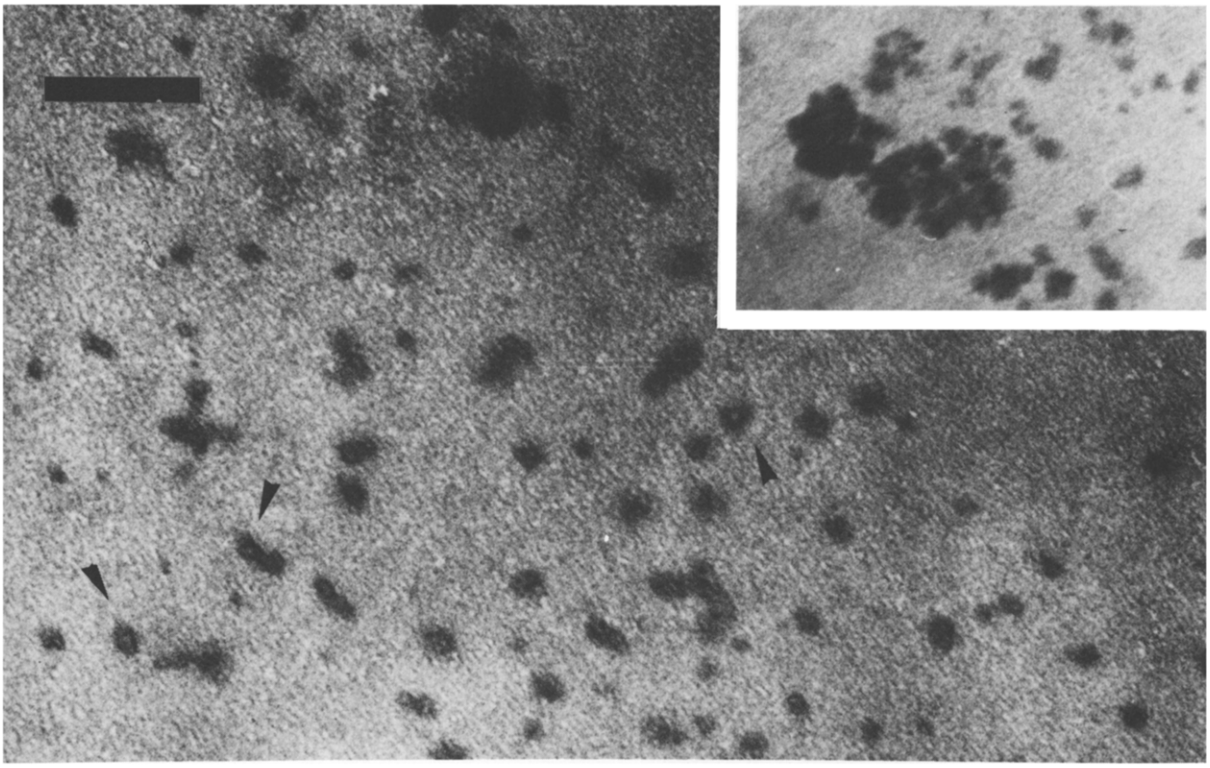

Fig. 1. Electron micrograph showing a typical field of NBD-aggregates embedded in Epon. Arrows mark structures which may represent sections from hollow spheres. Association of the NBD-aggregates to form larger assemblies is indicated by the appearance of large, generally spherical ensembles, shown in the inset. The bar represents 1000 Å.

metal ion stains used in the preparations (osmium and uranium) are generally considered to associate with the phosphate moieties of the phospholipids and thus the observed images probably represent headgroup assemblies. As shown in Fig. 1, small intact spheres with diameters between 50 and 350 Å (maximum population approx. 140 Å) as well as doughnut-shaped aggregates, which appear to represent cross sections through hollow spheres, were typical of the preparation. The different diameters of the aggregates can be explained by a size distribution of the intact aggregates and/or by the fact that the aggregates are sectioned at different levels. There is also evidence that these lipid aggregates form larger organizations with a spherical shape and having diameters between 300 and 1000 Å (see inset in Fig. 1).

(2) Negatively stained NBD-aggregates were generally spherical with a size range of 70–400 Å (Fig. 2). In agreement with the observations of aggregates included in Epon, the negatively stained aggregates had a maximum population with a diameter between 100 and 200 Å. Presumably, these aggregates represent a population deriving from larger organisations of particles such as those presented in the inset of Fig. 1.

Trilaminar profiles characteristic of bilayer structures were not detected by transmission EM in the *N*-NBD-DLPE samples. Using an average diameter of 100 Å and a surface area of 80 $Å^2$ for the particles, the total number of (I) in one aggregate was estimated to be 500.

(b) ^{31}P-NMR spectroscopy

^{31}P-NMR spectroscopy is a convenient method to study the polymorphic phase behaviour of phosphatidylethanolamines [25–27] Phospholipids in large hydrated bilayer structures give rise to broad asymmetric ^{31}P-NMR spectra with a low-field shoulder whereas phosphatidylethanolamines

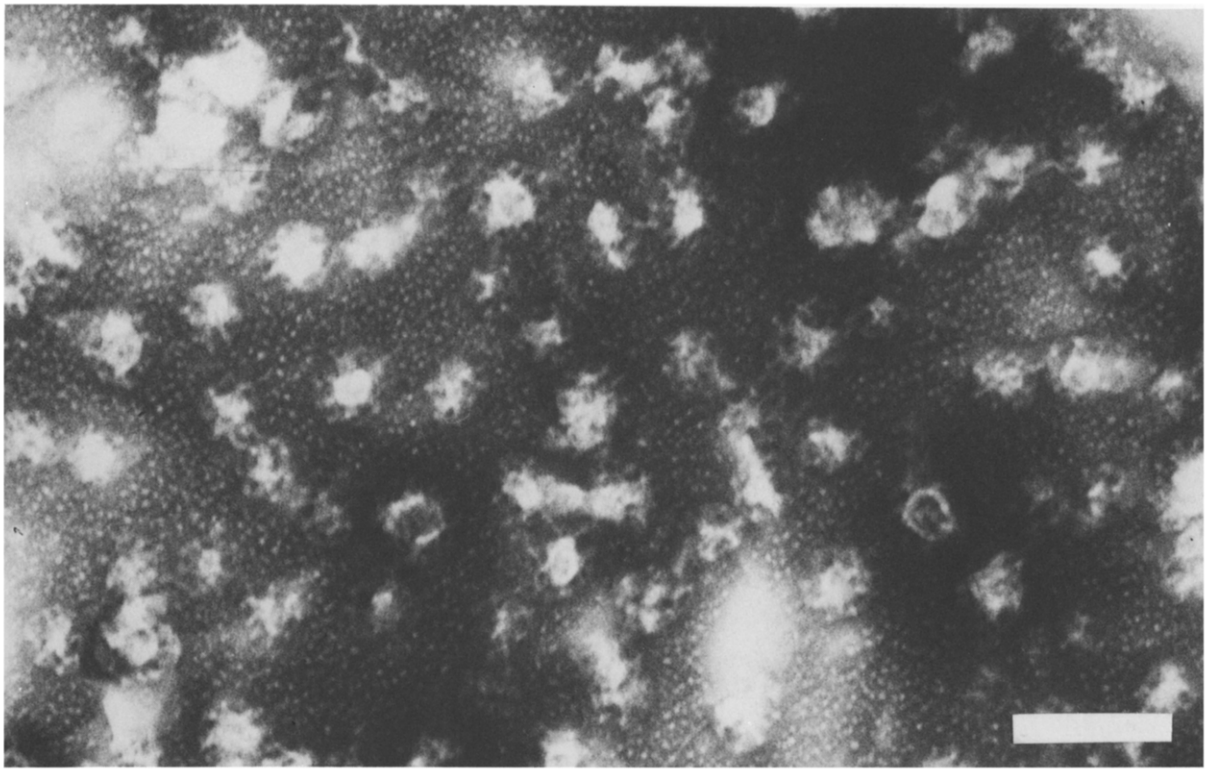

Fig. 2. Electron micrograph of negatively stained NBD-aggregates. The bar measures 1000 Å.

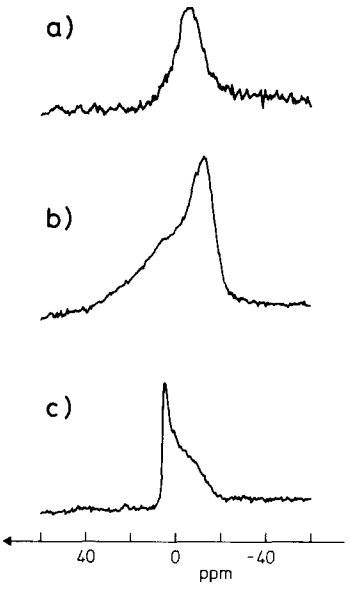

Fig. 3. ^{31}P-NMR spectra of hydrated samples of (a) (Ia), (b) DLPE and (c) PE from hen egg yolk at $T = 32°C$.

in the hexagonal (H_{II}) phase exhibit more narrow spectra with a high-field shoulder. Phospholipids in other available phases, e.g. cubic phases, exhibit much narrower symmetrical ^{31}P-NMR spectra [29,30]. In agreement with Cullis and De Kruijff [27] we obtained the characteristic ^{31}P-NMR spectra for DLPE (lamellar phase at 32°C) and for egg PE (hexagonal phase at 32°C) shown in Figs. 3b and 3c. In contrast to those results (Ia) gives rise to a ^{31}P-NMR spectrum (Fig. 3a) with much narrower bandwidth and a chemical shift value intermediate between those of the spectra in Figs. 3b and 3c. This shows that derivatization of the DLPE headgroup with NBD reduces the ability of the phospholipid to form ordered structures.

Ultracentrifugation

About 20% of the initial aggregates of (I) were pelleted at $100000 \times g$ (1 h). When the pellets were recentrifuged after addition of buffer, the same size-distribution as in the first centrifugation

step was obtained. This indicates the presence of an equilibrium of large and small aggregates in a ratio of 1 : 4 which is established in less than an hour.

Fluorescence decays of (I) in egg PC liposomes

The fluorescence properties of *N*-NBD-ethanolamine in ethanol-water mixtures are given in Table I. Increase in polarity of the solvent mixture leads to a bathochromic shift of the emission maximum while emission intensity and fluorescence decay time are reduced. While the fluorescence decays of *N*-NBD-ethanolamine in the ethanol-water mixtures were monoexponential and independent of emission wavelength, a sum of two exponential functions had to be applied to fit the fluorescence decays of (I) incorporated into egg PC liposomes. The mean lifetimes increase slightly towards the red edge of the emission spectrum (Table II) which is an indication for the contribution of solvent relaxation in the excited state [31,32] although ground state heterogeneity cannot be excluded.

It is known that the emission of NBD-labeled lipids incorporated into liposomes is extremely sensitive to self-quenching effects [11]. When increasing amounts of the compounds (I) were incorporated into liposomes the decay constants for both components decreased and the preexponential factors changed as indicated in Fig. 4. Compound (Ib) showed similar behaviour.

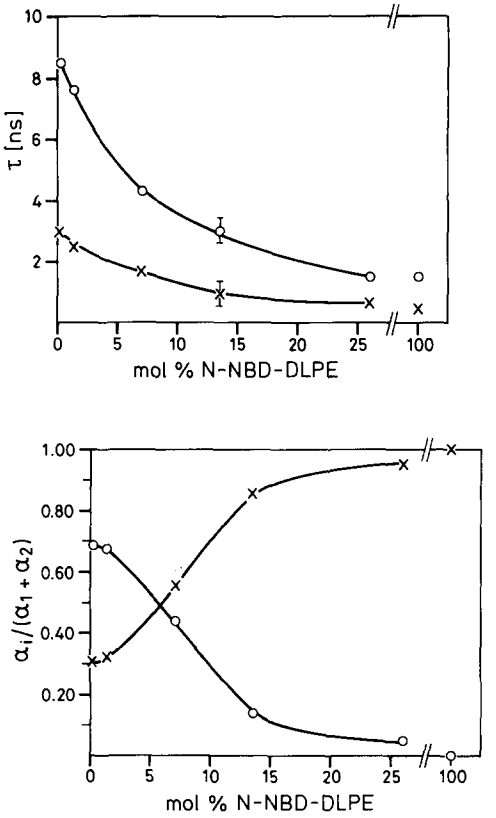

Fig. 4. Fluorescence decay parameters of (Ia) incorporated into LUV for various molar ratios of (Ia)/egg PC. (a) decay times, (b) preexponential factors.

Kinetic measurements of the incorporation of (Ia) into liposomes

(a) Influence of vesicle size. Liposomes were added to non-fluorescent aggregates of (I). The time-evolution of the steady-state emission inten-

TABLE I

EMISSION PROPERTIES OF *N*-NBD-ETHANOLAMINE IN MIXTURES OF ETHANOL-WATER

$5 \cdot 10^{-6}$ M, $\lambda_{exc} = 475$ nm for steady-state measurements, $\lambda_{exc} = 354$ nm for lifetime measurements.

% H_2O	λ_{max} (nm)	τ (ns)	Relative intensity
0	533	6.7	100
10	534	5.1	77
25	536	4.1	57
50	538	2.6	35
75	540	1.7	19
100	541	1.1	11

TABLE II

DEPENDENCE OF FLUORESCENCE DECAY PARAMETERS FOR (Ia) INCORPORATED INTO LUV ON THE EMISSION WAVELENGTH

$\lambda_{exc} = 354$ nm.

λ_{em} (nm)	τ_1 (ns)	τ_2 (ns)	α_1	α_2	$\langle\tau\rangle$ (ns)
493	1.7	8.4	0.15	0.09	6.8
535	2.8	8.5	0.06	0.09	7.4
554	3.3	8.3	0.08	0.18	7.7
573	3.4	8.5	0.08	0.17	7.7
593	3.8	8.6	0.05	0.11	7.8

sities of mixtures of (Ia) with SUV and with LUV during the first 70 min is given in Fig. 5a. The initial rate of increase in NBD emission intensity in mixtures of (Ia) with LUV is much faster than in mixtures with SUV. At later reaction times the intensities of the incubation mixtures become similar and reach identical equilibrium values after 2000 min. The behaviour of fluorescence lifetimes of the two mixtures is also different (Fig. 5b). When (Ia) is incorporated into LUV the mean lifetimes, $\langle\tau\rangle$, are constant over the whole time range shown in Fig. 5b. On the other hand, immediately after mixing a suspension of (Ia) with SUV the $\langle\tau\rangle$ values were significantly lower and showed a gradual increase in the first 60 min (Fig. 5b). Identical $\langle\tau\rangle$ values of 7.3 ns were obtained for both incubation mixtures in the equilibrium state. Similar behaviour as that described in Fig. 5 was observed also for (Ib). Fusion of SUV to larger vesicles under the influence of (I) was excluded by column chromatography and ultracentrifugation of the reaction mixtures after equilibration.

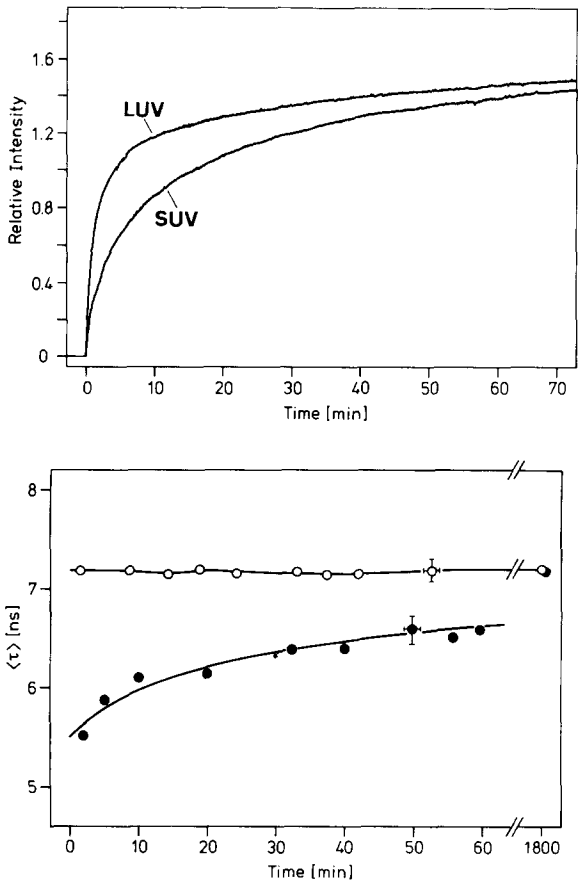

Fig. 5. (a) Time dependence of NBD-emission intensity in mixtures of *N*-NBD-DLPE aggregates ($5\cdot10^{-7}$ M) with SUV and with LUV ($2.5\cdot10^{-4}$ M) normalized by addition of Triton X-100. (b) Fluorescence decay times of the NBD group in mixtures of (Ia) with SUV (●) or LUV (○) at various reaction times.

(b) Influence of acyl chain length. In the following experiments we compared the time evolution of the steady-state emission intensities of mixtures of (Ia) and (Ib) with LUV (Fig. 6a). We distinguish a fast and a very slow kinetic component. (Fig. 6b). The data can be fitted by an equation the form

$$F(t) = a - b_1 \exp(-\gamma_1 t) - b_2 \exp(-\gamma_2 t) \qquad (3)$$

The γ values for (Ia) were significantly higher than those for (Ib) (see Table III). Besides the differences in the kinetic parameters we observed different equilibrium emission intensities F_{max} of the NBD group after approx. 2000 min. (Fig. 6 and Table IV). F_{max} and $\langle\tau\rangle$ have their highest values for the short-chain compound (Ia) and show a decrease with increasing length of acyl chains. The equilibrium values F_{max} and $\langle\tau\rangle$ obtained by incorporation of the aggregates of (Ia) and (Ib) were below the intensity values of $F = 2.2$ obtained by cosonication of the compounds with egg PC.

Variation of concentration

The fluorescence lifetimes for the equilibrium states after incorporation of the labeled lipids into

TABLE III

KINETIC PARAMETERS FOR THE INCORPORATION OF (Ia) AND (Ib) INTO LUV

Rate constants k_1–k_3 are calculated as described in text. The dimension of γ and k is min^{-1}. Values in brackets are half-times in min ($t_{1/2} = \ln 2/\gamma$ or $\ln 2/k$). Single standard deviations are approx. 10%.

	γ_1	γ_2	b_2/a	k_1	k_2	k_3
(Ia)	0.49	0.005	0.2	0.39	0.097	0.005
	(1.4)	(136)		(1.7)	(7.14)	(136)
(Ib)	0.15	0.002	0.56	0.067	0.083	0.002
	(4.62)	(346)		(10.3)	(8.3)	(346)

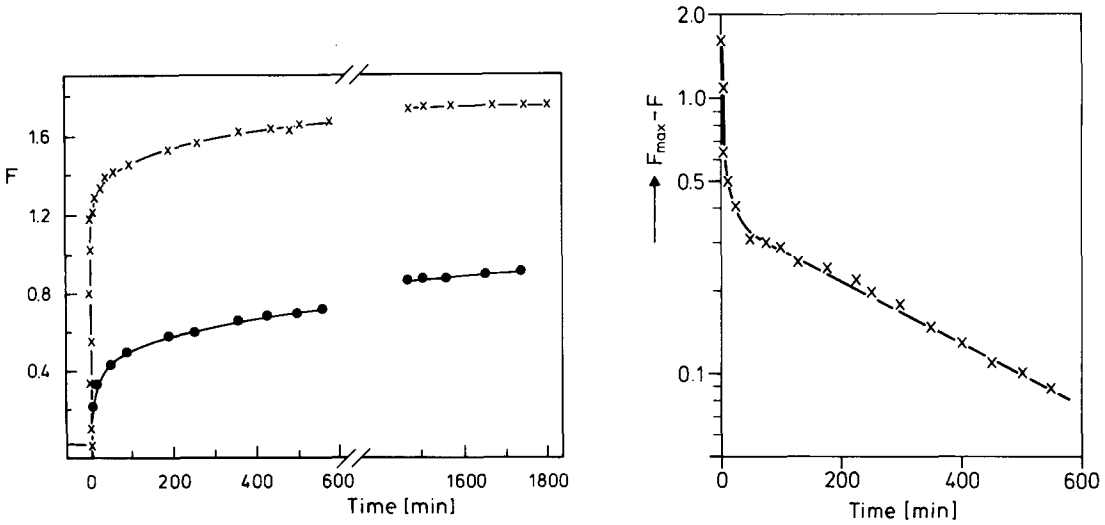

Fig. 6. (a) Time evolution of emission intensities in mixtures of (Ia) (×) and (Ib) (●) ($5 \cdot 10^{-7}$ M) with LUV ($2.5 \cdot 10^{-4}$ M). Emission intensities were normalized with respect to Triton-treated samples. (b) Logarithmic plot of intensity vs. reaction time for (Ia)/LUV.

LUV had to be fitted with sums of two exponential functions similar to those described in Table II. The mean values are given in Table IV. The plots in Figs. 5 and 6 were obtained from incubation mixtures containing $5 \cdot 10^{-7}$ M of (I) and $2.5 \cdot 10^{-4}$ M egg PC. Proportional decrease of the concentrations of both components down to values of $5 \cdot 10^{-8}$ M of (I) and $2.5 \cdot 10^{-5}$ M egg PC had no influence on the kinetic constants. However, for the mixtures with low concentrations lag times between zero time and the onset of the increase in emission intensity of several seconds were observed.

TABLE IV

EQUILIBRIUM EMISSION INTENSITIES F_{max} [a] AND MEAN FLUORESCENCE LIFETIMES $\langle\tau\rangle$ OF THE NBD GROUP FOR (Ia) AND (Ib)

	LUV [b]		Pellets [c]		Cosonicated [d]	
	F_{max}	τ (ns)	F_{max}	τ (ns)	F_{max}	τ (ns)
(Ia)	1.7	7.3	1.8	7.7	2.2	8.5
(Ib)	0.9	6.4	1.0	6.7	2.2	8.5

[a] Normalized with respect to the Triton X-100 treated samples. Mean lifetimes $\langle\tau\rangle$ of Triton-treated samples were 5.2 ± 0.2 ns independent of the hydrophobic part of (I).

[b] Incubation mixtures of (I) with LUV after 2000 min; $T = 23°C$.

[c] Fractions of LUV after incorporation of (Ia) and (Ib) pelleted by ultracentrifugation.

[d] Systems were produced by cosonication of (I) (0.2 mol%) with egg PC.

Ultracentrifugation of reaction mixtures in equilibrium state

The fact that the equilibrium emission intensity F_{max} is lower for (Ib) than for (Ia) gives rise to the question whether the extent of association of (I) with LUV decreases as a function of acyl chain length or whether the formation of non-fluorescent or weakly fluorescent states of (I) associated with LUV is favoured by increasing chain length.

In the first case, there should be free aggregates of (I) left in solution after equilibration and it should be possible to separate these from liposomes by ultracentrifugation. The emission intensities in the pelleted liposomes should be independent of fatty acid chain length of (I) and show a value close to that found for the cosonicated system ($F = 2.2$). However, if the second situation is encountered the pelleted samples should show differences in fluorescence intensities.

From the results given in Table IV we conclude that the extent of association of (I) with LUV is not influenced by the structure of the hydrophobic part of the labeled lipids. It is rather the average value of the fluorescence yield of the NBD moiety associated with the vesicles which is responsible for the different values of F_{max}.

Discussion

Kinetic measurements of the incorporation of (I) into egg PC vesicles of different size

Mutual interaction of lipid membranes may occur according to two extreme pathways depending on the reaction conditions, namely (i) transfer of phospholipids between bilayers through the aqueous phase via the monomer state [12–14,33,34] and (ii) fusion of membranes by direct contact [15–18].

In the present study we investigated the interaction of aggregates of NBD-labeled lipids with single bilayer egg PC membranes. According to EM and NMR experiments the labeled lipids are present in non-bilayer arrangements in aqueous suspension. The question arises whether these structures will interact with the egg PC bilayers via lipid transfer or via a fusion-like process where intact aggregates associate in a primary step with the vesicles.

The experimental results given in Fig. 5 show that there is a characteristic difference in the behaviour of fluorescence intensities and decay times in the mixtures of (I) with small and large egg PC vesicles. This is strong evidence for the interaction of whole aggregates of (I) rather than of monomers of labeled lipids with the vesicles in a primary step. The interaction of (I) with vesicles can be rationalized in a simple scheme (Scheme II).

$$
\begin{aligned}
&(\mathrm{I}) \quad + \mathrm{v} \rightarrow \mathrm{v}_1^* \qquad \text{(step 1)}\\
&\mathrm{v}_1^* \quad + \mathrm{v} \rightarrow \mathrm{v}_2^* \qquad \text{(step 2)}\\
&\qquad\qquad \vdots\\
&\mathrm{v}_{n-1}^* + \mathrm{v} \rightarrow \mathrm{v}_n^* \qquad \text{(step } n\text{)}
\end{aligned}
$$

Scheme II.

In step 1 the labeled lipid aggregates associate with unlabeled vesicles V (SUV or LUV) to give a fluorescent vesicle, v_1^*. Afterwards, in step 2 and the following steps labeled lipids are transferred from v_1^* to unlabeled vesicles v either as monomers or in a collision induced process. (A value of 37 min for the half-time of monomer transfer of (Ia) between SUV at 23°C has been determined [12]). After the incorporation of one aggregate of (I) (approx. 500 lipid molecules, see Results) into SUV (approx. 6000 lipid molecules) we obtain a molar concentration of (I) of approx. 8% while incorporation of the same amount of (I) into LUV (approx. 240000 lipid molecules) leads to a concentration of approx. 0.2%. Due to the strong self-quenching effects in v_1^* in the case of SUV (see Fig. 4), steps 2 to n will lead to an increase in lifetimes. For the mixture of (I) with LUV steps 2 to n will also occur. However, emission intensities are not reduced by self-quenching in V_1^* at short incubation times. Therefore, the fluorescence lifetimes have reached the equilibrium values of $\langle\tau\rangle \approx 7.3$ ns at reaction times of several minutes already. For the same reasons the emission intensities for the SUV will be significantly lower in the first period of the reaction than for mixtures containing LUV. Gradually intensities as well as mean lifetimes reach identical values (Fig. 5).

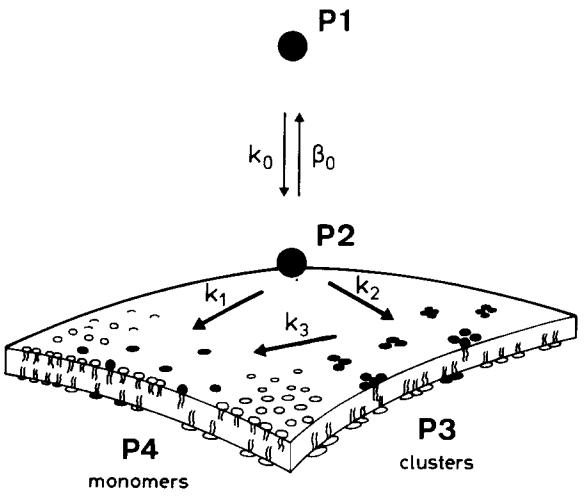

Fig. 7. Kinetic model for the incorporation of (I) into liposomes (model 1).

Kinetic model

In order to exclude complications arising from the self-quenching effects in the case of SUV we restrict the discussion to the interaction of (I) with LUV only. The two main facts resulting from Figs. 5 and 6 and Table IV are: (i) While the NBD fluorescence lifetimes are constant for incubation mixtures of (Ia) and (Ib) for reaction times from several minutes up to 2000 min, the increase in emission intensity is biphasic. (ii) The equilibrium emission intensity F_{max} is lower for the incorpora-

TABLE V

A. KINETIC MODELS COMBINING TWO NON-FLUORESCENT POOLS AND A FLUORESCENT ONE

Subscripts D and F indicate non-fluorescent and fluorescent pools, respectively.

Model		Initial population	Fit with experiment
2a	$(P1)_D \overset{k_1}{\rightarrow} (P2)_D \overset{k_2}{\rightarrow} (P3)_F$	P1 (C_1^0)	not possible
2b		P1 and P2 (C_1^0, C_2^0)	possible
3a	$(P1)_D \underset{\beta_1}{\overset{k_1}{\rightleftharpoons}} (P2)_D \overset{k_2}{\rightarrow} (P3)_F$	P1 (C_1^0)	not possible
3b		P1 and P2 (C_1^0 and C_2^0)	possible
4	$(P1)_D \overset{k_1}{\searrow}$ $(P3)_F$ $(P2)_D \overset{k_2}{\nearrow}$	P1 and P2 (C_2^0 and C_2^0)	possible

B. ALGEBRAIC SOLUTIONS FOR MODELS 2–4

The solutions were obtained using the operator method as described in the Appendix. C_1^0, C_2^0 are initial concentrations (at $t = 0$) and $C_T = C_1^0 + C_2^0$.

$R_1 = -P_1$ and $R_2 = -P_2$ are the roots of the expression $P^2 + P(k_1 + k_2 + \beta_1) + k_1 k_2 = 0$.

Model	Solution
2a	$F(t) = fC_1^0[1 - \frac{k_2}{k_2 - k_1} e^{-k_1 t} - \frac{k_1}{k_1 - k_2} e^{-k_2 t}]$
2b	$F(t) = f[C_T - k_2 \frac{C_T - C_2^0}{k_2 - k_1} e^{-k_1 t} - \frac{C_T k_1 - C_2^0 k_2}{k_1 - k_2} e^{-k_2 t}]$
3a	$F(t) = fC_1^0 k_1 k_2 [\frac{1}{R_1 R_2} - \frac{1}{R_1(R_2 - R_1)} e^{-R_1 t} - \frac{1}{R_2(R_1 - R_2)} e^{-R_2 t}]$
3b	$F(t) = f[C_T - \frac{C_T R_2 - C_2^0 k_2}{R_2 - R_1} e^{-R_1 t} - \frac{C_T R_1 - C_2^0 k_2}{R_1 - R_2} e^{-R_2 t}]$
4	$F(t) = f[C_T - C_1^0 e^{-k_1 t} - C_2^0 e^{-k_2 t}]$

tion of (Ib) than for (Ia). Ultracentrifugation experiments showed that this is due to weakly fluorescent or non-fluorescent states preferentially formed by compound (Ib) and irreversibly associated with the liposomes. This drop in emission intensity with increase in acyl chain length was not observed for cosonicated systems: Intensities and lifetimes of compounds (Ia) and (Ib) were identical ($F_{max} = 2.2$, $\langle \tau \rangle = 8.5$ ns) when incorporated into LUV by cosonication with egg PC (Table IV).

Biphasic or even more complex kinetics have been obtained for the incorporation of small fluorescent molecules like ANS [6–9] as well as for a headgroup labeled phospholipid [10] into liposomes. The occurrence of more than one kinetic phase has been assumed to be due to the presence of two different kinds of fluorescent binding sites, such as, for example, attachment of the fluorescent molecules to the membrane surface in a fast step followed by penetration into the hydrophobic interior in a slow step [6–8]. Such a two-site model with two fluorescent pools would not be able to explain the difference in the behaviour of the fluorescence lifetimes observed during the incorporation of (I) into SUV and into LUV. It

would lead to monoexponential increase in emission intensity accompanied by increase in fluorescence decay times with progressive incorporation of the labeled lipids. Obviously this does not fit our experimental results. If we modify the model assuming the existence of a non-fluorescent pool and another one emitting with a lifetime of 7.3 ns we would obtain fluorescence decays independent of the state of label incorporation. However, the increase in emission intensity would be monoexponential. This means that a kinetic model which fits our data has to be more complex.

Therefore we suggest the reaction scheme depicted in Fig. 7 (model 1). In the first collision-mediated step, small aggregates of (I) adhere to the surface of liposomes. This step is concentration dependent and it is responsible for the lag-time periods observed for low concentrations of the components of the incubation mixtures. In the following steps the aggregates of (I) dissolve into two pools as indicated in Fig. 7. The phase transition temperature of saturated phosphatidylethanolamines are significantly higher than that of egg PC ($T_p = 29°C$ for DLPE, 47.5°C for DMPE [35]). Although the phase transition temperatures for the labeled compounds (I) are not known we may assume that at 23°C their hydrophobic part is in the gel state. Therefore, we expect clusters of solid phosphatidylethanolamines (I) in the liquid egg PC matrix [36]. It is reasonable to assume that these clusters are non-fluorescent due to self-quenching effects. According to Fig. 7 they slowly dissociate into monomers. The concentrations of *N*-NBD-labeled lipids in the four different kinetic pools (P1–P4) are given by C_1–C_4. k_0, β_0, k_1, k_2 and k_3 are the rate constants for the transitions between the four states.

The collision-mediated step in which aggregates of (I) adhere to the liposome surface is a fast process and therefore it can be neglected in the evaluation of the long-time effects. The pool P2 in Fig. 7 will be considered as the starting pool for the incorporation process.

Therefore, penetration of NBD-lipids into LUV can be described by the following system of differential equations:

$$dC_2/dt = -(k_1 + k_2)C_2 \tag{4a}$$

$$dC_3/dt = k_2C_2 - k_3C_3 \tag{4b}$$

$$dC_4/dt = k_1C_2 + k_3C_3 \tag{4c}$$

Eqns. 4a–4c were solved by the operator method [37] (see Appendix). The measured steady-state emission is the contribution from kinetic pool P4

$$F(t) = fC_4 \tag{5}$$

where f is the correlation factor between fluorescence intensities and the concentrations of (I) in P4. From Eqn. 5 and the expression for C_4 given by A-5c (see Appendix) we obtain Eqn. 6 for the increase of fluorescence intensity:

$$F(t) = \alpha - \alpha_1 e^{-(k_1+k_2)t} - \alpha_2 e^{-k_3 t} \tag{6}$$

where,

$$\alpha = C_2^0 f \tag{6a}$$

$$\alpha_1 = C_2^0 f(k_1 - k_3)/(k_1 + k_2 - k_3) \tag{6b}$$

$$\alpha_2 = C_2^0 f k_2/(k_1 + k_2 - k_3) \tag{6c}$$

C_2^0 is the starting concentration in pool P2.

By comparing Eqns. 6 and 3 we obtain the three rate constants:

$$k_1 = \gamma_1 - (\gamma_1 - \gamma_2)(b_2/a) \tag{7a}$$

$$k_2 = (\gamma_1 - \gamma_2)(b_2/a) \tag{7b}$$

$$k_3 = \gamma_2 \tag{7c}$$

Values for k_i obtained from Eqns. 7 are shown in Table III.

Generally speaking the simplest model to explain double-exponential increase of emission intensities (Eqn. 3) accompanied by constant fluorescence lifetime requires the contribution of two non-fluorescent pools and a fluorescent one. In model 1 we suggest that those pools (P2–P4) are all located in the membrane and that they are connected by reactions with rate constants k_1–k_3. To obtain a more general view of the situation in Table V we present variations of the model together with their algebraic solutions. In model 2 P1–P3 are linked by two consecutive reactions. For the case that at zero time all labeled lipids are concentrated in P1, the model is not in agreement with the experimental results because the signs for the two preexponentials are opposite (compare

preexponentials in Table VB for model 2a). However, when at zero time the NBD-labeled lipids are present in P1 and P2 mathematical agreement between model and experiment is possible. The situation for model 3 is similar while the only version of model 4 is in agreement with the experiment.

As far as the physical significance of models 2b, 3b and 4 is concerned it is hardly conceivable that two kinetically non-equivalent, non-fluorescent pools $(P1)_D$ and $(P2)_D$ are formed within the membrane by interaction with the aggregates of (I) at zero time.

A second situation which has to be considered is the location of the non-fluorescent pools in the aqueous phase of the incubation mixtures. This can be excluded, however, from the observation that none of the rate constants was dependent on the concentration of (I) and of liposomes in the solutions. Further centrifugation experiments (Table IV) showed that the nonfluorescent lipids could be pelleted, indicating that the nonfluorescent pools are associated with liposomes. Therefore, by exclusion of the variations 2–4 we come to the conclusion that model 1 (Fig. 7) gives the best explanation of the experimental results.

Influence of the hydrophobic part of (I) on kinetic parameters and on equilibrium emission intensities

We have shown that the half-times for the increase in emission intensity (γ values in Eqn. 4) as well as the rate constants k_1–k_3 were lower for the incorporation of compound (Ib) than for that of (Ia).

In terms of model 1 this means that the non-fluorescent clusters P2 and P3 dissolve more slowly in the egg PC matrix when the fatty acids of the labeled lipids are increasing in length.

As far as the lower value of equilibrium emission intensity F_{max} of (Ib) as compared to that of (Ia) is concerned (Table IV) there are two possible explanations. The first one assumes that the total distribution of compounds (I) as monomers in the membranes is inhibited by equilibria between the pools P3 and P4. In the case of (Ia) the equilibrium would be shifted more towards the monomers P4 than for the case of Ib. The second explanation would assume that besides the pools depicted in Fig. 7 we have to expect non-fluorescent aggregates of (I) associated with the liposomes which cannot be removed by ultracentrifugation, and do not participate in the incorporation reactions given in model 1. They are formed to a much higher extent in the incubation mixtures of (Ib) with LUV as compared to those containing (Ia) (Table IV).

Both assumptions lead to the conclusion that increase in acyl chain length of (I) leads to lower degree of homogeneity of membrane structures.

Reorganization of membrane structures

One of the main conclusions from these results is that upon adsorption of the aggregates of (I) to the liposomes a high degree of heterogeneity has been created in the membrane. By our measurements we were able to study the relaxation of this heterogeneous state towards a more homogeneous lipid distribution. It was not possible to study this type of relaxation phenomena by conventional methods of fluorescence labeling. Such equilibration processes might be important in biological problems like e.g. membrane biogenesis or mixing of membrane regions by fusion. Fluorescence measurements using self-quenching effects as presented in this work should be suited to gain insight into those processes.

Appendix

The solutions of the differential Eqns. 4a–4c were obtained using the operator method. In this method the differentials d/dt are replaced by the operator P:

$$\frac{dC}{dt} = PC \text{ for } C(t=0) = 0 \qquad \text{(A-1)}$$

$$\frac{dC}{dt} = PC - PC^0 \text{ for } C(t=0) = C^0 \neq 0 \qquad \text{(A-2)}$$

Combining Eqns. A-1 and A-2 with Eqn. 3 we obtain:

$$(P + k_1 + k_2)C_2 = PC_2^0 \qquad \text{(A-3a)}$$

$$-k_2C_2 + (P + k_3)C_3 = 0 \qquad \text{(A-3b)}$$

$$-k_1C_2 - k_3C_3 + PC_4 = 0 \qquad \text{(A-3c)}$$

This system of three linear equations with the

unknowns C_i can be solved using Cramer's rule treating the operator P as a constant. The determinant of the system A-3 is

$$\Delta = P(P + k_1 + k_2)(P + k_3) \tag{A-4}$$

The expressions obtained for C_1, C_2 and C_3 are functions of the operator P and can be transformed to original functions by a reverse Laplace-Carson transformation using the Tables of Transforms in Ref. 37. The complete set of solutions is given in Eqns. A-5:

$$C_2 = C_2^0 \, e^{-(k_1+k_2)t} \tag{A-5a}$$

$$C_3 = C_2^0 k_2 \left[\frac{1}{k_3 - k_1 - k_2} e^{-(k_1+k_2)t} + \frac{1}{k_1 + k_2 - k_3} e^{-k_3 t} \right] \tag{A-5b}$$

$$C_4 = C_2^0 \left[1 - \frac{k_1 - k_3}{k_1 + k_2 - k_3} e^{-(k_1+k_2)t} - \frac{k_2}{k_1 + k_2 - k_3} e^{-k_3 t} \right] \tag{A-5c}$$

From Eqns.A-5c and 5 a double-exponential function for the increase of the fluorescence intensity is obtained (Eqns. 6 and 7).

Acknowledgements

We thank Dr. A.R. Holzwarth, Max-Planck-Institut für Strahlenchemie, for valuable help with analysis of fluorescence decays. One of us, A.C., thanks La Ligue National Française Contre le Cancer for financial support and the CNRS, Orléans for the possibility of using the EM equipment. Skilfull technical assistance by Ms. E. Hüttel is gratefully acknowledged.

References

1 Yguerabide, J. and Foster, M.C. (1981) in Membrane Spectroscopy (Grell, E., ed.) pp. 199–269, Springer, Berlin
2 Inbar, M. and Shinitzky, M. (1974) Proc. Natl. Acad. Sci. USA 71, 2128–2130
3 Zachariasse, K.A., Vaz, W.L.C., Sotomayor, C. and Kuehnle, W. (1982) Biochim. Biophys. Acta 688, 323–332
4 Almeida, L.M., Vaz, W.L.C., Zachariasse, K.A. and Madeira, V.M.C. (1982) Biochemistry 21, 5972–5977
5 Golan, D.E., Alecio, M.R., Veatch, W.R. and Rando, R.R. (1984) Biochemistry 23, 332–339
6 Tsong, T.Y. (1975) Biochemistry 14, 5409–5414
7 Tsong, T.Y. (1975) Biochemistry 14, 5415–5417
8 Haynes, D.H., Staerk, H. (1974) J. Membrane Biol. 17, 313–340
9 Moss, R.A., Hendrickson, T.F., Swarup, S., Hui, Y., Marky, L. and Breslauer, K.J. (1984) Tetrahedron Lett. 25, 4063–4066
10 Sunamoto, J., Nomura, T. and Okamoto, H. (1980) Bull. Chem. Soc. Jap. 53, 2768–2772
11 Hoekstra, D. (1982) Biochemistry 21, 1055–1061
12 Arvinte, T. and Hildenbrand, K. (1984) Biochim. Biophys. Acta 775, 86–94
13 Nichols, J.W. and Pagano, R.E. (1981) Biochemistry 20, 2783–2789
14 Nichols, J.W. and Pagano, R.E. (1982) Biochemistry 21, 1720–1726
15 Vanderwerf, P. and Ullman, E.F. (1980) Biochim. Biophys. Acta 596, 302–314
16 Struck, D.K., Hoekstra, D. and Pagano, R.E. (1981) Biochemistry 20, 4093–4099
17 Hoekstra, D. (1982) Biochemistry 21, 2833–2840
18 Ababei, L. and Hildenbrand, K. (1984) Chem. Phys. Lipids 35, 39–48
19 Monti, J.A., Christian, S.T. and Shaw, W.A. (1978) J. Lipid Res. 19, 222–228
20 Huang, C.H. (1969) Biochemistry 8, 344–352
21 Zumbuehl, O. and Weder, H.G. (1981) Biochim. Biophys. Acta 640, 252–262
22 Cornell, B.A., Middlehurst, J. and Separic, F. (1980) Biochim. Biophys. Acta 598, 405–410
Small, D.M. (1967) J. Lip. Res. 8, 551–557
23 Knight, A.E.W. and Selinger, B.K. (1973) Austr. J. Chem. 26, 1–27
24 Inokuti, M. and Hirayama, F. (1965) J. Chem. Phys. 43, 1978–1989
25 Cullis, P.R. and De Kruijff, B. (1976) Biochim. Biophys. Acta 436, 523–540
26 Cullis, P.R., Van Dijck, P.W.M., De Kruijff, B. and De Gier, J. (1978) Biochim. Biophys. Acta 513, 21–30
27 Cullis, P.R. and De Kruiff, B. (1978) Biochim. Biophys. Acta 513, 31–42
28 Cullis, P.R. and Hope, M.J. (1978) Nature 271, 672–674
29 Rilfors, L., Khan, A., Brentel, I., Wieslander, A. and Lindblom, G. (1982) FEBS Lett. 149, 293–298
30 Eriksson, P.-O., Lindblom, G. and Arvidson, G. (1985) J. Phys. Chem. 89, 1050–1053
31 DeToma, R.P., Easter, J.H. and Brand, L. (1976) J. Am. Chem. Soc. 98, 5001–5007
32 DeToma, R.P. (1983) in Time-Resolved Fluorescence Spectroscopy in Biochemistry and Biology (Cundall, R.B. and Dale, R.E., eds.), pp. 393–410, Plenum Press, New York
33 Nakagawa, T. (1974) Colloid Polym. Sci. 252, 56–64
34 Duckwitz-Peterlein, G., Eilenberger, G. and Overath, P. (1977) Biochim. Biophys. Acta 469, 311–325
35 Van Dijck, P.W.M., De Kruijff, B., Van Deenen, L.L.M., De Gier, J. and Demel, R.A. (1976) Biochim. Biophys. Acta 445, 576–587
36 Shimshick, E.J. and McConnell, H.M. (1973) Biochemistry 12, 2351–2360
37 Rodiguin, N.M. and Rodiguina, E.N. (1964) Consecutive Chemical Reactions, Mathematical Analysis and Development, Van Nostrand, Princeton, NJ